



Conception of a Salinity-Gradient Solar Pond in Beirut, Lebanon: Instrumentation, Control, Maintenance and Economic

Khawla Sleiman^{1,2}, Stefan Van Vaerenbergh¹, Tayssir Hamieh^{2,3*}

¹ Microgravity Research Center, Université libre de Bruxelles (ULB) - Service de Chimie Physique, Brussels B1050, Belgium

² Laboratory of Materials, Catalysis, Environment and Analytical Methods Laboratory (MCEMA), Faculty of Sciences, Lebanese University, Hadath 6573/14, Lebanon

³ Faculty of Science and Engineering, Maastricht University, P.O. Box 616, Maastricht 6200 MD, Netherlands

Corresponding Author Email: t.hamieh@maastrichtuniversity.nl

Copyright: ©2022 IIETA. This article is published by IIETA and is licensed under the CC BY 4.0 license (<http://creativecommons.org/licenses/by/4.0/>).

<https://doi.org/10.18280/psees.060101>

ABSTRACT

Received: 4 August 2022

Revised: 4 September 2022

Accepted: 10 November 2022

Available online: 31 December 2022

Keywords:

solar ponds, renewable energy, conception and control

Lebanon, currently engulfed in a severe economic crisis, grapples with substantial challenges in electricity provisioning due to systemic grid failures, foreign dependence, depleting resources, and the costly adoption of fossil fuels. These exigencies necessitate a shift towards innovative, renewable energy solutions, thereby positioning Salinity-Gradient Solar Ponds (SGSPs) – artificial reservoirs harnessing and storing solar energy – as a potentially effective response. This study proffers an instrumented engineering proposal advocating the implementation of SGSPs in Lebanon, detailing the operational management, control, and maintenance required for reliable heat production. By articulating the feasibility and benefits of SGSPs within the Lebanese context, the paper underscores their potential to alleviate existing energy constraints and foster a more sustainable, self-sufficient energy future for the nation.

1. INTRODUCTION

The pervasive economic crisis Lebanon is currently navigating, exacerbated by the catastrophic explosion in the port of Beirut on August 4, 2020, has underscored the urgent need for reformation in the country's energy sector. The state-run electricity provider, Électricité du Liban (EDL), is mired in allegations of corruption and mismanagement, leaving citizens grappling with frequent power outages that can exceed 20 hours a day in some regions. The implications of these power shortages reverberate through the economy, precipitating inflated energy bills and necessitating the advent of alternative electricity generation and distribution methods. Private generators, while resolving issues of access, impose substantial costs that often exceed the financial capabilities of many citizens. Additionally, the lack of resources has stymied attempts at restructuring the sector and implementing crucial reforms, further exacerbated by a reliance on imported oil products to fulfill 94% of the country's consumption. Biomass, coal, and primary electricity account for a meager 2% each, underscoring the dire need for a paradigm shift in Lebanon's energy infrastructure.

In this climate of increasing global complexity and rising fossil fuel costs, the search for new, effective, and sustainable energy sources has become paramount. Solar energy systems have emerged as a promising solution to address both human and industrial energy demands. Despite their potential, existing solar technologies such as thermodynamic solar power plants, evacuated tube solar thermal collectors, and photovoltaic cells present significant barriers in terms of high

costs and extensive maintenance requirements. These are primarily attributed to the need for separate systems for the collection and storage of solar radiation.

In contrast, solar ponds offer a cost-effective and low-maintenance alternative. These thermal devices, by simultaneously collecting and storing solar energy, have been identified as low-cost investments that require minimal maintenance [1, 2]. Distinguished by their high energy storage capacity and the stability of their energy supply, solar ponds absorb solar radiation, which subsequently heats the water in their lower layers. Under normal circumstances, this heated water would rise to the surface and release its heat to the surroundings. However, by increasing the salt concentration in the bottom layer, the water becomes denser, thus preventing convection and retaining 20 to 30% of the absorbed heat [3-5]. This results in a temperature gradient between the bottom and the surface, defining the unique characteristics of Salinity-Gradient Solar Ponds (SGSPs).

2. SGSP PRINCIPLE

SGSP is formed from three layers of brine of different concentrations (Figure 1): (i) The first layer on the top of the pond is called the Upper Convective Zone (UCZ). It has the lowest temperature - close to ambient temperature - and salinity - about 5-10 % - and must have the lowest thickness since it is directly exposed to atmospheric influences, then it will not really affect the stability of the pond. (ii) The non-convective zone (NCZ) is the layer isolating the lower zone in

which the heat will be stored. It is characterized by a critical thickness depending on the temperature to be reached in the pond, the water thermal conductance and the solar transmission properties. Its salinity and temperature increase with depth. iii) The bottom layer called the lower convective zone (LCZ) or the heat storage zone (HSZ) has the highest temperature - up to 95°C; salinity - around 26% - and thickness which will determine the amount of heat which can be stored to benefit from in winter or cloudy days and nights [6].

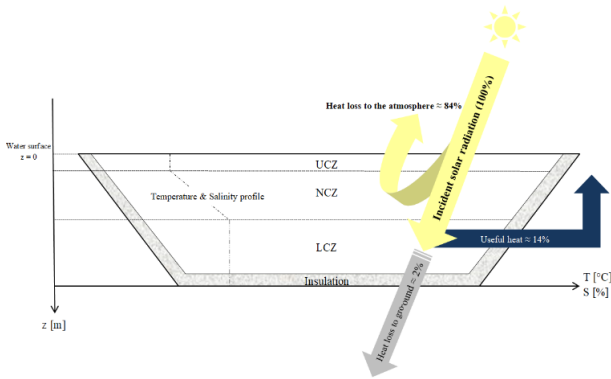


Figure 1. Schematic of SGSP layers, temperature and salinity profile, and solar energy distribution

3. SGSP PROPOSED PROJECT

To build an SGSP, the following factors must be taken into account: large areas of flat inexpensive land, a good annual average of solar radiation, minimal normal wind speeds, a source of fresh water and large quantities of suitable salt near the pond. The Mediterranean Sea region can meet these requirements, which makes Beirut - the capital of Lebanon - a suitable place to implement this technology.

3.1 Geographical location characteristics

The behavior of any thermal sensor is influenced by its geographic and meteorological location. Therefore, solar ponds should be built in a hot and humid climate. Located along the southeastern shoreline of the Mediterranean Sea, Beirut has a hot-summer Mediterranean climate characterized by mild days and nights. As its benefits from favorable climatic conditions (Table 1, Figures 2 and 3), the SGSPs will have great potential in the production of electricity and the industrial applications.

And considering the geographical characteristics of Lebanon (Figure 4), it would be effective to mention the geographical factor which contributes to the stability of the temperature, throughout the year, in the pond which will thus

respond to any constant demand of heat: if the water table under the basin is deep, the ground will act as an additional heat storage volume [7]. However, a pond with at least 5m of water below is highly recommended to minimize heat loss to the ground.

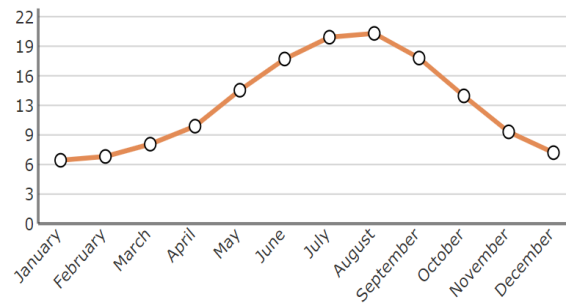


Figure 2. Absolute humidity in g/m³, in Beirut

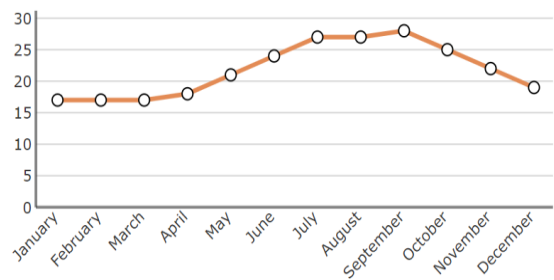


Figure 3. Water temperatures in °C, in Beirut

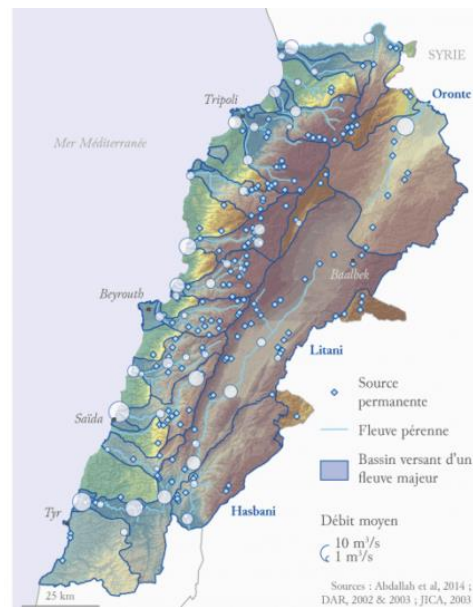


Figure 4. Lebanon water-table map

Table 1. Geographical and meteorological data for Beirut

Coordinates	33° 53' 20" N, 35° 29' 40" E											
Altitude [m]	0											
Summer maximum temperature [°C]	35											
Winter minimum temperature [°C]	12											
	January	February	March	April	May	June	July	August	September	October	November	December
Average ambient temperature [°C]	14	14	16	19	22	25	27	28	27	24	20	16
Daylight [h]	10	11	12	13	14	14	14	13	12	11	10	10
Average solar insolation [kWh/m²/day]	3	3	5	6	7	8	8	7	6	4	3	2
Wind average speed [m/s]	4	4	4	3	3	3	3	3	3	3	3	4

3.2 Sizes and applications

To determine the surface area of a solar pond to be built, it is first necessary to specify: the desired average annual temperature of this pond, the average annual ambient temperature, the annual insolation and the latitude. As the desired average pond temperature increases, the surface area of the pond must increase; unlike the annual average ambient temperature and insolation. Their increases guarantee the desirability of a smaller solar pond. On the other hand, to minimize heat loss on the edges of the pond, it is preferable to maximize the ratio between the surface of the pond and its perimeter. Therefore, a small pond will not be as effective as a larger one. Thus, for residential heating applications for example, it will be preferable to build a large pond for a group of dwellings, rather than to build a small pond for each dwelling. As for the latitude, it indicates the average elevation angle of the sun, hence the surface reflection losses which are greater at higher latitudes. And with a high probability of a drop in ambient temperature and insolation, the surface of the pond therefore tends to increase with increasing latitude [8].

A 1,000 m² SGSP will be suitable for space heating and cooling, greenhouse and swimming pool heating, crop drying and various industrial applications requiring low quality heat such as dairy plants, water desalination and salt production. In Australia, Alice Springs pond verified that the 2,000 m² experimental salinity-gradient solar ponds, via a Rankine cycle engine, could generate 20 kW (e) [9]. A 3,000 m² solar pond coupled with a desalination plant, near the Dead Sea, provided an annual average production rate of 4.3 L/min distilled water [10]. A computer simulation of a 10,000 m² and 3 m deep solar pond proposed to be built in Sabzevar, Iran, proved that around 59,000 MJ/day of thermal energy can be extracted from the pond in June; thus methane saving of approximately 1,576 kg/day [11]. Large-area SGSPs, i.e. over 100,000 m² in area, have proven manageable and practical for power generation in the order of 5 MW (e) using the Rankine organic fluid cycle [12-17].

3.3 Conception

To test the SGSPs effectiveness in alleviating the burden of the energy crisis in Lebanon, a 3,000 m² square solar pond with 3 m depth and 45° inclined walls [18], can be launched in Beirut as a first step; and its contribution to covering the energy needs of industrial sectors can be studied. The solar pond can provide process heat to industry, significantly saving the need for oil, electricity, coal and natural gas. Thermal energy can be beneficial in manufacturing by industrial heating, either for the preparation of materials and objects, or for their treatment, or both processes together [19]. According to results, it is possible to work to develop the application of this technology and benefit from it in other Lebanese regions that meet the geographical and climatic conditions of the SGSPs. The electricity production is discussed later (Section 7).

3.4 Conventional projects to benefit from

3.4.1 El paso solar pond project

The El Paso Solar Pond is a 3,000 m² SGSP located on the wealth of Bruce Foods, Inc. (Figure 5), launched in 1983 and operated by the University of Texas since 1985. It was

approximately 3.25 m deep with UCZ, NCZ and LCZ layers 0.7 m, 1.2 m and 1.35 m thick, respectively. The LCZ contained saturated or nearly saturated sodium chloride (NaCl) brine, with a concentration of approximately 26% by weight. The concentration in the UCZ was maintained at 10,000-41,000 mg/L. The pond, operating in a temperature range of 77-87°C, provided hot water for the food factory and generated electricity via a 100 kW power system, and was used for a multi-stage flash evaporation unit to desalinate water afterwards.

The pond was decommissioned in late 2003. During its 16 years of operation, the 3 essential applications of salinity gradient solar ponds (electricity generation, process heat supply and fresh water supply) have been proven there. Its economic analysis showed that SGSPs depend on the following 3 factors: the local geographical and meteorological conditions, the size of the pond (the larger the pond, the more economically feasible it will be) and the desired applications [20].



Figure 5. The El paso solar pond

3.4.2 Pyramid hill solar pond project

The Pyramid Hill Solar Pond, a 3,000 m² pond built at Pyramid Salt's facilities at Pyramid Hill in northern Victoria, Australia (Figure 6), has demonstrated that SGSPs are an innovative and lucrative, collecting and storing solar energy technique for other applications such as heating and power generation. It was 2.3 m deep, positioned approximately 200 m from the Pyramid Hill salt production plant, to minimize heat loss. During its 7 years of operation, it has provided heat for use in the production of high quality salt, aquaculture – especially the production of brine shrimp for stock feed – and thermal desalination. The planned requirement of heat was 60 kW. The heating system has been dedicated to the production of salt in its final crystallization phase, supplying it with hot air at around 45°C [21].



Figure 6. The pyramid hill solar pond

4. CONSTRUCTION

4.1 Coating

A great success has been found with coatings of small-scale solar ponds in plastic materials. However, this was not the case for larger than 5 km² solar ponds, used for power production, because the use of these materials will increase the cost of the pond by 30%. However, using clay liners instead would reduce the cost of construction and the hot brine contamination risk of groundwater and subsoil [22].

4.1.1 El paso solar pond

The pond experienced coating failures [23]: In 1984, PVC coated polyester fabric with a finished weight of 1 kg/m² was installed as part of a double coating system, with an existing hypalon liner underneath to form secondary liner [24]. The projected life of this coating was 20 years; while after 7 years of operation of the pond, more than 100 holes have been identified on the lining of the lower side walls exposed to high temperatures. The material strength deteriorated to 10% of its original strength [25]. Then, tests on five compacted local clays were carried out in order to determine their mineralogical composition, optimal compaction and hydraulic conductivity. But none of the compacted clay liner (CCL) systems withstood the environmental conditions of the pond.



Figure 7. Flexible polypropylene geomembrane liner installation



Figure 8. Geotextile installation

In 1994, a Geosynthetic Clay Liner (GCL) - a 0.2" sodium bentonite clay layer containing 92% montmorillonite, to resist the effects of brine contamination; glued to 30 mil polypropylene, with a free swell of 31 ml per 2 g dry matter – and a flexible polypropylene geomembrane - the sidewall liner sewn from 40 mil polypropylene and installed over a secondary containment liner of 30 mil polypropylene - were installed at the bottom of the pond (Figures 7-9), the GCL with

the clay side down to minimize contact between the bentonite and the brine and separated from the polypropylene by a layer of geotextile to protect it. The GCL seams were covered by 30 to 50 cm and a cover of 146 kg/m² of sand was installed. Under the GCL, a drainage system was installed to monitor the leakage rate [26]. However, an improper UV stabilizer incorporated into the resin material during the manufacture of the liner caused the liner to degrade on the sides of the pond under UV exposure, after 2 years of installation. As a result, the pond was drained and lined with an upgraded 60 mil polypropylene liner that had held up until late 2003.



Figure 9. Liner system installed

4.1.2 Pyramid hill solar pond

Due to its ability to resist to saturated brine at temperatures up to 100°C and UV rays, a 1 mm thick Nylex Millennium polypropylene liner was used to cover the pond. A sump has been created at the northeast corner of the bottom, to monitor the liner condition and a pipe has been introduced under the liner to control the sump water level which indicates whether the liner is broken-down. Since borehole observations showed that the aquifer level at the Pyramid Hill site was approximately 3m from the ground surface, five groundwater quality levels and quality below the pond, monitoring stations were installed under the liner and four stations around the pond, and a 100 mm thick expanded polystyrene (EPS) insulation was used at the bottom of the pond to reduce average heat loss by 42% [21, 27].

4.2 Heat extraction system

Energy extraction is the process that unites all SGSPs, regardless of the application for which they were designed, and is carried out using two methods: (i) the first method used for large-scale applications, such as the El Paso Solar Pond and Bhuj 6,000 m² Solar Pond, consists of an extraction diffuser mounted in the LCZ to pump hot brine to an external heat exchanger, before it returns to the LCZ by means of a return diffuser (Figure 10). (ii) In the second method used for different sizes ponds, such as a 4 m² pond at Ferdowsi University in Mashhad, a 200 m² pond at Ohio State University and the Pyramid Hill solar pond, the cold working fluid inside the coiled pipes of an internal heat exchanger, installed in the LCZ near the NCZ, transfers thermal energy from the hot brine to an external heat exchanger (Figure 11).

4.2.1 El paso solar pond

For its effectiveness, the first method was used exclusively for heat extraction, as already mentioned above. Two diffusers were placed close to the point of use: the extraction one at the LCZ maximum temperature height, and the return one below,

which guarantees the return of the cold brine downwards, and therefore the ground losses reduction. These diffusers consisted of a 1.9 cm polypropylene plate and a 15 cm rubber hose that connected them to the external piping system. The extraction diffuser was mounted under the apron of an instrumentation tower 20 cm below the lower limit and the return diffuser about 15 m from the tower (Figures 12 and 13). A winch and a cable attached to the extraction diffuser made it possible to adjust it. A brine removal rate of 600 US gallons/min was achieved [21].

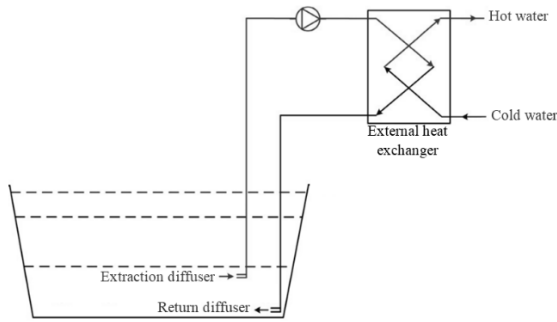


Figure 10. Schematic of diffusers and external heat exchanger

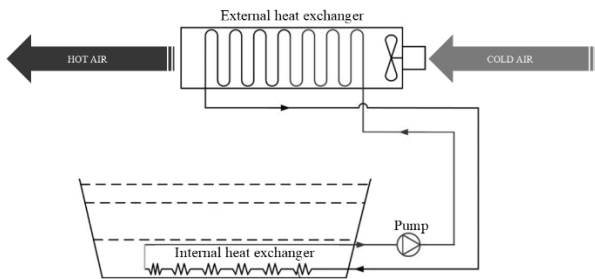


Figure 11. Schematic of internal and external heat exchangers



Figure 12. Instrumentation tower

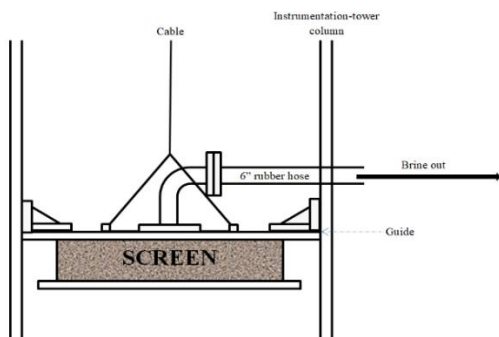


Figure 13. Suction-diffuser schematic

4.2.2 Pyramid hill solar pond

Fresh water circulated through Iplex Poliplex BlueLine Medium Density Polyethylene (MDPE 80 B) plastic tubing (26 mm ID, 31 mm OD) located in the LCZ, just below the NCZ-LCZ interface, from the heat exchanger, then heated, passed through a 200 m second heat exchanger to extract heat via a 1.5 kW centrifugal pump. The heat exchanger which supplies hot air to the salt production process was a cross-flow liquid-air heat exchanger with copper tubes and aluminum fins, designed for a 60 kW output with a 174 LPM water flow rate.



Figure 14. Heat extraction tubes connected to polyethylene manifold pipes



Figure 15. Heat extraction tubes insulated and inserted in larger plastic tubes



Figure 16. Expansion tank

To resist corrosion, the tubes of the heat exchanger have been made with plastic, thus guiding towards a practical low thermal conductivity ($0.37 \text{ W/m}^\circ\text{C}$). To compensate for this, an increase in the heat exchange surface was adopted by laying forty-eight 60 m long tubes connected to two polyethylene collectors (ID 72.9 mm, DE 90 mm) manufactured in the same material and insulated with 40 mm expanded polystyrene (Figure 14). Since the density of saturated brine is greater than

that of fresh water and plastic pipes, the tubes were under upward pressure and were therefore attached to plastic covered dumbbells installed prior to the construction of the salinity profile to hold them in place. To prevent heat loss from the working fluid, the tubes were insulated via 9mm thick Armaflex insulation (32mm ID) and larger plastic tubes (56.8mm ID, 63mm OD) inserted on the insulation, from the start of the NCZ to the manifold ports (Figure 15) [21]. To charge the heat extraction system with fresh water and allow expansion during operation, an open 1,000 L capacity expansion tank (Figure 16) made of polyethylene linear low density (LLDPE) and wrapped in polystyrene foam insulation, was placed 2.5 m above the floor [21].

4.3 Instrumentation

For the proper functioning of an SGSP, reliable instrumentation will be essential, and samplings of critical parameters, such as temperature, density, pH and turbidity, will have to be taken, monitored and analyzed regularly.

Temperature and density profiles are the most direct and easiest ways to know the UCZ-NCZ and NCZ-LCZ interfaces. The conventional way of measuring can be summarized as follows: Temperatures at different heights of the entire pond must be measured, every 2 seconds, by tens of thermo-resistors distributed at constant intervals. Then 10 minute, hourly, daily and monthly averages should be recorded. An automatic weather station will measure, every 10 seconds, the ambient temperature – as well as other meteorological data such as solar radiation, wind speed, relative humidity, etc. Next, hourly, daily and monthly averages of ambient temperature should also be recorded. Density, pH and turbidity will be measured respectively by a density meter, pH meter and turbidimeter. And to check the salt-gradient stability, samples will have to be taken at different LCZ positions, constantly distant.

In the next two sections, noteworthy and more detailed instrumentation and monitoring procedures are presented.

4.3.1 El paso solar pond

Using scanner technology and a computer controlled data logger, an automated and integrated instrumentation system – comprising: (i) a sensor head mounted on a drum cable scanner which, with a pump sampler, were together mounted on the instrument tower deck (Figure 12); (ii) a "U" tube hydrometer, turbidimeter, pH probe and cooling heat exchanger mounted on the edge of the pond near the instrumentation tower, all in the same enclosure; (iii) a control and data logging computer, installed in an instrumentation room adjacent to the pond – was specially developed for the pond and characterized by the power to simultaneously measure temperature, salinity and brine quality in about 3 hours, thus ensuring an almost “real-time” view of the state of the pond, in order to properly maintain the gradient. Via a stepper motor and a computer that precisely controlled the depth, the reliable and precise scanner offered high spatial resolution, continuous data collection and easy management. The collector head – which served as the extraction diffuser and through which the brine samples pass to the heat exchanger, and the devices mounted on the edge of the pond – was cut in the middle so as to form a 0.2 cm semi-circular inlet space; two of its opposite faces are mounted by two T-type thermocouples providing redundancy; and a counterweight was fitted to its bottom, to overcome its buoyancy in heavy brine and allow the scanner to descend

more easily [28, 29].

4.3.2 Pyramid hill solar pond

Twenty resistance temperature detector (RTD) sensors were attached, at 10 cm intervals in UCZ and NCZ and at 20 cm intervals in LCZ, to a pole to form the automatic pond monitoring system (Figure 17). They were connected to a data logger programmed to record data from each sensor every 10 s and the hourly average of each parameter. An additional salinity, pH and turbidity sampling tube was attached to a pole whose level could be changed in the pond for regular manual sampling to monitor the stability of the NCZ [21].



Figure 17. Poles on which RTD sensors and sampling tube were attached

4.4 Methods to enhance SGSP efficiency

Solar ponds can provide reliable thermal energy at temperatures ranging from 20 to 90°C [30]. But, practically and taking into account the meteorological, geographical and operational difficulties affecting the good performance of the pond, it is difficult to reach a temperature higher than 70°C [5]. Therefore, to enhance the efficiency of SGSP, different methods have been presented by many researchers:

4.4.1 Floating rings

Air velocity plays an important role in the stability of the salinity gradient, because surface currents can mix the layers and disturb the gradient, thus reducing the efficiency of heat extraction. Therefore, a minimum of speed will be desired. Research on heat pipe heat exchangers (HPHE) has shown that thermal efficiency will increase significantly if the average air velocity is reduced from 5 to 1 m/s [31]. To suppress wave action, high density polyethylene (HDPE) rings 1.5 mm thick and 35 mm wide can be placed on the UCZ which will then be divided into small isolated cells [21, 32]. This is the case of the surface of the Pyramid Hill Solar Pond (Figure 6), where a number of flat strips 74 mm wide; 4 mm thick and 5 m long were fixed to each other via hose clamps and floating polyvinyl chloride (PVC) pipes [21].



Figure 18. Light reflectors

4.4.2 Light reflectors and solar covers

The rate of heat collected and stored in the pond directly depends on the surface first exposed to the sun. Two components can be effective in increasing energy storage for better heat extraction: reflectors (Figure 18) which will help control the reflection of solar rays in such a way as to increase the rate of incident rays through the top surface, and the solar covers (Figure 19) that will be used to retain the heat in the pond. Their use, together, leads to a considerable increase in the rate of stored heat [33].



Figure 19. Solar covers

4.4.3 Flat plate solar collectors

The flat plate collector converts solar energy into heat much faster than the solar pond. But unfortunately, in the absence of a storage system, the collected heat will be lost if it is not used within a few days. While the solar pond has the advantage of the large capacity to store it for long periods. Therefore, a system coupling these two solar collectors can improve energy efficiency.

A study showed that the maximum and minimum thermal efficiencies of a conventional solar pond and an integrated solar pond supported by conventional solar collectors, for the month of August, were 28.41% and 33.55%, respectively; and that the efficiency of the conventional solar pond and the integrated solar pond, for January, decreased to 8.3% and 9.5%, respectively [34]. Another study confirmed the increase in thermal and electrical performance and in the generation of hydrogen by Organic Rankine Cycle (ORC), up to 25 kg of

hydrogen per day, when the solar pond was integrated with four flat plate solar collectors [35]. An experiment carried out in Barcelona, Spain, on a cylindrical pond 300 cm high and 800 cm in diameter integrated with four 10 m² solar collectors confirmed that the use of solar collectors as an external heat source for the solar pond results in a 50% increase in total thermal efficiency [36].

4.4.4 Evacuated tube solar collectors

The use of evacuated tube solar collectors improves the energy and exergy performance of a solar pond. These performances for solar ponds without collectors can reach 10.4% and 4.3% respectively, whereas for a pond with a configuration of solar collectors with four vacuum tubes, 16.94% and 10.3%, respectively [37]. In order to increase the thermal mass of an SGSP, evacuated tube solar collectors were used as an external heat source, proving a 35 and 30% increase in annual efficiency and average annual heat extraction, respectively [38].

5. OPERATION

To establish a salinity gradient, a quantity of suitable salt must be dissolved in the pond. Salinity, therefore, varies from near zero at the surface to high levels at the bottom of the pond. Thus, by preventing vertical convection, the salt gradient helps retain solar heat at the bottom.

5.1 Salt selection

A suitable salt should verify the following criteria: (i) High solubility value to ensure high solution densities. (ii) Solubility insensitive to temperature. (iii) Solution sufficiently transparent to solar radiation. (iv) Safe to handle and environmentally friendly salt [3]. The most commonly used salt is NaCl, because it strongly meets the previous criteria (Table 2). But more important than its physical properties, is that the salt is widely available near the pond so that its transport costs do not dominate its low purchase costs; especially since a quantity of suitable salt of the order of half to several tons per square meter of pond will be necessary and therefore the cost of salt will strongly invade the economy of the SGSP [39].

Table 2. Thermal properties of aqueous solutions of NaCl [40]

T [°C]	S [%]	$\nu(\times 10^{-9})$ [m ² /s]	$\kappa_s(\times 10^{-9})$ [m ² /s]	$\kappa_s(\times 10^{-7})$ [m ² /s]	$\alpha(\times 10^{-4})$ [°C ⁻¹]	$\beta(\times 10^{-3})$ [m ³ /kg]
40	0	0.66	2.26	1.52	4.2	0.69
	5	0.68	2.1	1.54	3.9	0.65
	10	0.73	2.14	1.56	4.4	0.62
	15	0.82	2.19	1.57	5.2	0.59
	20	0.89	2.26	1.56	5.5	0.56
50	0	0.56	2.77	1.56	4.6	0.68
	5	0.58	2.57	1.58	4.3	0.65
	10	0.62	2.63	1.6	4.6	0.62
	15	0.66	2.68	1.61	4.9	0.59
	20	0.74	2.77	1.6	5.2	0.56
60	0	0.48	3.3	1.59	5.4	0.67
	5	0.51	3.07	1.61	4.9	0.64
	10	0.55	3.15	1.64	5	0.61
	15	0.58	3.23	1.64	5	0.58
	20	0.63	3.3	1.63	5	0.55

5.2 Salt-gradient establishment

The NCZ is the most important layer of an SGSP. A crucial step in this technology comes down to the stability of this zone, and establishing a salinity gradient profile will thus be a sensitive task on which much research has been carried out [41-43]. As a result, the best and most common technique for constructing the salinity gradient; even for the construction of the temperature gradient, was found to be the water injection method [41, 44]. In this method, the pond is first partially filled (volume of the LCZ + half of the remaining volume [45]) with concentrated brine. Then, using a diffuser [44], the salinity gradient is adjusted by injecting low saline water at the NCZ-LCZ interface. This task should be done gradually to achieve balance in the layer. The fixed-level injection process must be controlled by the dimensionless Froude number representing the ratio of kinetic energy to gravitational potential energy of the injection fluid. It can be calculated using the following equation [46]:

$$Fr = \frac{\rho v^2}{\Delta \rho g B} \quad (1)$$

where, ρ is the density of the surrounding saline fluid, in kg/m^3 ; v the injection velocity at the diffuser outlet, in m/s ; g the acceleration due to gravity, in m/s^2 ; $\Delta \rho$ the density difference between the injected fluid and the surrounding fluid, in kg/m^3 ; and B the gap width of the diffuser, in m [44]. The Froude number must be maintained at a constant value of approximately 18, in order to obtain complete mixing at the level of the injection diffuser [42, 43]. If it is lower than this value, the injected fluid rises by buoyancy and mixes above the level of the diffuser. If it is larger, the injected fluid carries large amounts of fluid below the level of the diffuser. To satisfy the Froude number requirement, the flow rate and diffuser geometry must be adjusted to match changes in ambient fluid density at each injection stage. Therefore, the space of the injection diffuser must be adjusted frequently [14]. The diffuser gap is usually about 2-3 mm [41], and is limited to 10-20 mm [14].

Gradual injections of low-salt water continue up to the NCZ-UCZ interface. Finally, fresh water will be injected on the surface using a floating system to avoid any mixing.

5.2.1 El paso solar pond

The previous method was used at the pond, but the process of constructing the gradient was costing time and labor. Therefore, a scanning injection technique was successfully adapted in 1995 [29]. Instead of staying at a set level, the diffuser was continuously moved up and down within a small predefined range – for El Paso, 20 cm for all; but the last five steps, smaller ranges were used – called “scan range”.

This procedure can be divided into five steps: 1. Design the pond configuration: pond depth, zones' thicknesses and desired salinity profile (more details in reference [41]). 2. Estimate the mass of needed salt. 3. Plan the injection process in several stages: for each injection stage, determine the lower limit (which is the elevation of the LCZ-NCZ interface, for the first injection stage) that will be increased by approximately 5 cm for each consecutive step, the upper limit and the volume of water to be injected according to the desired salinity profile, its distribution since the previous injection step and the water and salt balances. 4. Inject until the designed upper limit of NCZ is reached. 5. Add fresh water to the surface through a

floating diffuser to avoid mixing, until the intended water level is reached.

Comparison between fixed level injection and scanning injection. The technique offers the following advantages: (i) Much smoother resulting salinity profile and more precise matching to the desired one. (ii) Easier to use, less labor intensive and less time consuming – 50% faster, for El Paso. (iii) Not as sensitive to the Froude number – the only requirement is that the injection rate be sufficient to achieve a minimum Froude number of 18 to ensure adequate mixing [21].

Material, instrumentation and control. For gradient establishment before 1995, circular double-plate diffusers were used away from the banks or the instrument tower, to avoid interference. In 1995, a tubular diffuser was installed on the instrument tower for use in gradient construction, consisting of two PVC pipes of 10 cm diameter and equal length, glued to a tee connected to the fresh water line by a 3 inch rubber hose, and over which were 14 slots 3.8 cm long and 0.32 cm wide, spaced 2.5 cm apart. A DC motor and drum-cable system mounted below the instrument tower bridge drives the movement of the diffuser and a precision potentiometer operates as a position feedback system, so that when the diffuser reaches the preset limit, a computer automatically reverses the motor direction. At the end of an injection step, the lower and upper limits could be reset for the next injection [21].

5.2.2 Pyramid hill solar pond

To establish the gradient, consecutive layers of brines of different salinities from the existing Pyramid Salt evaporation ponds were superimposed from the top layer, in a batch method. A semi-circular diffuser, 600 m in diameter, made of 316 stainless steel and mounted 5 cm above the bed of the pond ensures the injection of the bottom layers (Figure 20).



Figure 20. Semi-circular diffuser

6. MAINTENANCE

During the SGSP operation, different parameters such as NCZ boundary and gradient stability, salt management, clarity and thermal performance should be analyzed and controlled routinely, to guarantee the gradient zone stability, then, a good performance of the solar pond.

6.1 Boundary positions and internal stability

To get the salinity or temperature distribution equation in the gradient boundary-region, in the aim of locating the boundary positions, the curve was fitted with only the four data NCZ points adjacent to the boundary.

The NCZ stability was indicated by the Stability Margin Number (SMN) which must be greater than 1. For less than 1.6 at a given depth, a gradient break occurs [47]. A value of 2.5 is the operational safety limit near which corrective measures must be introduced to maintain the NCZ stability. SMN is defined as the the measured stability coefficient ratio to the calculated stability coefficient required to satisfy the dynamic stability criterion [41, 47, 48], and expressed mathematically as:

$$SMN = \left(\frac{dS_a}{dz} \right) \left(\frac{dS_j}{dz} \right) \quad (2)$$

where, dS_a/dz is the actual salinity gradient (in % salt/m), as computed from measured values, and dS_j/dz the indicated theoretical salinity gradient value (in % salt/m) required to satisfy the dynamic stability criterion for the given (measured) temperature profile at height z within the gradient zone [21].

6.2 Water level and salt loss

The downward and upward movements of the upper and lower boundaries, respectively, represent a natural consequence of surface water evaporation, erosion caused by convection, and upward salt transport by diffusion. This unfortunately induces a decrease in the thickness of the NCZ. Thus to maintain a better thickness of this zone, the UCZ must be diluted by frequent addition of fresh water – rinsing using a hose, in order to avoid surface disturbances and consequently the destabilization of the gradient – while increasing the saturation of the LCZ, by employing salt chargers to replenish the salt in the bottom area. And since the water level in the pond must be fixed, an overflow system must drain excess water from the surface.

At the Pyramid Hill Solar Pond, approximately 0.5 m³ of concentrated brine or 130 kg of bittern's magnesium chloride (a salt production by-product from salt water evaporation, the density of which may be greater than 1,300 kg/m³ against 1,200 kg/m³ for sodium chloride aqueous solutions) is added daily to the LCZ, through orifices whose heights determine the position of the NCZ lower interface, of a salt loader of 1.2 m in diameter and 3 m high (Figure 17). On the other hand, at three separate points, the surface of the pond was rinsed with approximately 30 m³/day of low-salt drilling water (3-4%), i.e. at a rate twice higher than the water loss by evaporation. Excess water went into an adjacent evaporation pond for salt production [21].

6.3 Clarity system

Maintaining good transparency with low turbidity is essential to increase the penetration of solar radiation into the LCZ, and thus the thermal efficiency and stability of the pond. Since clarity is usually contaminated by algae growth, bacteria, and dirt that falling in – leaves, organic matter, industrial particles, sand, and fine dust, an acidification system must be installed to regulate the pH and prevent algae growth. Low turbidity should be achieved by constantly keeping the water

pH below 3 [45] in both the NCZ and UCZ, by pH level weekly monitoring. Hydrochloric acid (HCl) is generally used for this purpose. A volume of the brine is extracted and acidified with a volume of hydrochloric acid equal to one-fourth of the volume extracted. The acidified solution will then be re-injected into the layer that is experiencing algae growth due to the low pH environment. However, injection of the acidic solution into the vicinity of the LCZ-NCZ interface should be avoided, as crystallization will occur when a saturated NaCl-brine solution reacts with HCl [45].

Either, at Pyramid Hill a natural approach was taken to maintain clarity and avoid the use of chemicals, by adding brine shrimp that feed on algae and detritus [21].

6.4 Thermal performance

Models have been developed [16, 49-61] to analyze the thermal performance of an SGSP through two complementary thermodynamic tools: energy analysis based on the first law of thermodynamics, which accounts energy in quantity and ignores its qualitative aspects [62] – by estimating the absorption rates of incident solar radiation and the heat transfer in the three pond-zones; then, exergy analysis based on the second law, which represents the qualitative as well as the quantitative aspects of the energy.

6.4.1 Energy analysis

Experimental, theoretical and numerical investigations was presented to determine the thermal performance of SGSPs in their different layers and under different conditions.

A study carried out on an isolated solar pond during the months of January, May and August, at day and night, showed that the total heat losses from the inner surface, the bottom and the side walls, in depending on the temperature difference, was 227.76 MJ [61]. A large amount of predicted heat loss between day and night presents significant potential for energy and storage savings. The temperature difference was found to be the main driving force of heat transfer. The highest thermal efficiency was achieved for August as follows: 4.5% for UCZ, 13.8% for NCZ, and 28.1% for LSZ, respectively [60]. In a 50 m² circular pond, the maximum temperature was observed at the NCZ, then it decreased at the LCZ due to the absence of adequate insulation of the slab, thus preventing the good heat storage in the LCZ [44]. Sidewall shading effects must be taken into consideration when thermally analyzing small solar ponds, because the pond's storage efficiency increases by eliminating these effects [57]. However, they are negligible for large solar ponds. An experimental study carried out on a small rectangular solar pond showed that the highest energy yields, in the month of August, in the cases of presence and absence of shading zone, were respectively equal to: 4.22% and 4.30% for UCZ, 13.79% and 16.58% for NCZ, and 28.11% and 37.25% for LCZ [63]. And the shading effect ratios were: 0.651 in the LCZ, 0.279 in the NCZ and 0.068 in the UCZ. The thermal performance of a solar pond is further affected by turbidity. The collection efficiency of the solar pond decreases with increasing turbidity [64]. The extraction of heat from the NCZ, in addition to or instead of the LCZ, can increase the energy efficiency of a solar pond by up to 50% [65] and even 55% [21] compared to the conventional method of extracting heat exclusively from the LCZ. This is attributed to the reduction of conductive heat loss to the UCZ. Another experimental and theoretical study on the process of extracting heat from the LCZ of a 7 m² experimental solar pond, using a

heat exchanger heat pipe (HPHE) and varying the velocity of the intake air used to extract heat from the condenser end of the HPHE, showed a 43% increase in efficiency when the air velocity decreased from 5 m/s to 1 m/s [31].

Then, to determine the thermal performance of the SGSP, energy-efficiency can be presented as the ratio of net energy transfer Q_{net} to the energy input to the system Q_{in} [60]:

$$\eta_e = \frac{Q_{net}}{Q_{in}} \quad (3)$$

UCZ thermal efficiency. The net heat Q_{net} i.e. stored heat Q_{stored} in the UCZ comes from: the amount of net, absorbed solar-radiation Q_{solar} by the UCZ and the total heat transferred from the lower zone NCZ to the UCZ, Q_{NCZ} ; excluding heat losses to the sidewalls of the pond $Q_{sidewalls}$ and heat losses from the upper surface to the surroundings $Q_{surrounding}$. Then the equation of the energy balance of the UCZ can be written as follows:

$$\begin{aligned} Q_{net,UCZ} &= Q_{stored,UCZ} \\ &= (Q_{in} - Q_{out})_{UCZ} \\ &= (Q_{solar} + Q_{NCZ})_{UCZ} - (Q_{sidewalls} + Q_{surrounding})_{UCZ} \end{aligned} \quad (4)$$

The thermal efficiency of the UCZ is obtained by plugging the Eq. (4) in the Eq. (3):

$$\eta_{e,UCZ} = \left(1 - \frac{Q_{sidewalls} + Q_{surrounding}}{Q_{solar} + Q_{NCZ}} \right)_{UCZ} \quad (5)$$

NCZ thermal efficiency. The net heat Q_{net} i.e. stored heat Q_{stored} in the NCZ comes from: the amount of net, transmitted solar-radiation Q_{solar} from the UCZ and the total heat transferred from the lower zone LCZ to the NCZ, Q_{LCZ} ; excluding heat losses to the sidewalls $Q_{sidewalls}$ and heat losses to the UCZ, Q_{UCZ} . Then the equation of the energy balance of the NCZ can be written as follows:

$$\begin{aligned} Q_{net,NCZ} &= Q_{stored,NCZ} \\ &= (Q_{in} - Q_{out})_{NCZ} \\ &= (Q_{solar} + Q_{LCZ})_{NCZ} - (Q_{sidewalls} + Q_{UCZ})_{NCZ} \end{aligned} \quad (6)$$

The thermal efficiency of the NCZ is obtained by plugging the Eq. (6) in the Eq. (3):

$$\eta_{e,NCZ} = \left(1 - \frac{Q_{sidewalls} + Q_{UCZ}}{Q_{solar} + Q_{LCZ}} \right)_{NCZ} \quad (7)$$

LCZ thermal efficiency. The net heat Q_{net} i.e. stored heat Q_{stored} in the LCZ comes from the amount of attenuated, transmitted solar-radiation Q_{solar} from the UCZ and the NCZ, excluding the heat losses the bottom Q_{bottom} , heat losses to the sidewalls $Q_{sidewalls}$ and heat losses to the NCZ, Q_{NCZ} . Then the equation of the energy balance of the LCZ can be written as follows:

$$\begin{aligned} Q_{net,LCZ} &= Q_{stored,LCZ} \\ &= (Q_{in} - Q_{out})_{LCZ} \\ &= Q_{solar,LCZ} - (Q_{bottom} + Q_{sidewalls} + Q_{NCZ})_{LCZ} \end{aligned} \quad (8)$$

The thermal efficiency of the LCZ is obtained by plugging the Eq. (8) in the Eq. (3):

$$\eta_{e,LCZ} = \left(1 - \frac{Q_{bottom} + Q_{sidewalls} + Q_{NCZ}}{Q_{solar}} \right)_{LCZ} \quad (9)$$

6.4.2 Exergy analysis

An efficient energy system requires - in addition to the energy analysis - an exergy analysis that takes into account the design of the system, its optimization and the improvement of its performance. This analysis allows the thermodynamic evaluation of energy conservation in energy systems by distinguishing between energy losses in the environment and internal irreversibilities in the processes (exergy destruction). It locates and characterizes the causes of exergy destruction or exergy losses, and quantifies the corresponding rates. A general exergy balance can be expressed in the following form [1]:

$$\begin{aligned} \text{Exergy input} - \text{Exergy output (useful and losses)} &= \\ \text{Exergy accumulation} + \text{Exergy consumption or} & \text{destruction} \end{aligned} \quad (10)$$

Exergy efficiency of a system or individual zone is defined as the the desired exergy output ratio - net UCZ and NCZ exergy transfer as useful product, or exergy accumulation in case of LCZ stored heat - to the exergy input to the system or individual zone [1]:

$$\eta_{ex} = \frac{Ex_{out,desired}}{Ex_{in}} \quad (11)$$

Solar radiation exergy. Thermal radiation from the sun is relatively rich in exergy. Then, exergy of the solar radiation in watt (W) on the top surface of solar pond can be written as follows:

$$Ex_{Solar} = G_S \left[1 + \frac{1}{3} \left(\frac{T_0}{T_S} \right)^4 - \frac{4}{3} \left(\frac{T_0}{T_S} \right) \right] A \quad (12)$$

where, G_S is the rate of incident solar radiation, in W/m²; T_0 the environment reference temperature, in K; and T_S the surface temperature of the sun (=6000 K).

Heat transfer exergy. The exergy of heat transfer - internal and external heat transfer of solar pond per unit area - is expressed by the following general equation:

$$Ex_Q = Q \left(1 - \frac{T_0}{T} \right) \quad (13)$$

where, Q is the heat transfer, in W; T the temperature of the system / individual zone, in K.

UCZ exergy efficiency. The desired exergy output from the UCZ comes from the exergy of solar radiation reaching the

UCZ, Ex_{solar} and the exergy gained from the NCZ, $Ex_{Q,NCZ}$; excluding the exergy loss from the UCZ to the surroundings, $Ex_{Q,surrounding}$, the exergy loss through the UCZ sidewalls, $Ex_{Q,sidewalls}$ and the exergy destruction in the UCZ, $Ex_{Q,destruction}$. Then, the equation of the exergy balance for the UCZ can be written as follows:

$$\begin{aligned} Ex_{out,UCZ} &= [Ex_{in} - (Ex_{losses} + Ex_{destruction})]_{UCZ} \\ &= \left[\begin{array}{c} Ex_{solar} + Ex_{Q,NCZ} \\ - (Ex_{Q,surrounding} + Ex_{Q,sidewalls}) \\ - Ex_{Q,destruction} \end{array} \right]_{UCZ} \end{aligned} \quad (14)$$

The exergy efficiency of the UCZ is obtained by plugging the Eq. (14) in the Eq. (11):

$$\eta_{ex,UCZ} = \left(1 - \frac{Ex_{Q,surrounding} + Ex_{Q,sidewalls} + Ex_{Q,destruction}}{Ex_{solar} + Ex_{Q,NCZ}} \right)_{UCZ} \quad (15)$$

NCZ exergy efficiency. The desired exergy output from the NCZ comes from the exergy transferred from the UCZ to the NCZ, $Ex_{out,UCZ}$ and the exergy gained from the LCZ, $Ex_{Q,LCZ}$; excluding the exergy loss from the NCZ to the UCZ, $Ex_{Q,UCZ}$, the exergy loss through the NCZ sidewalls, $Ex_{Q,sidewalls}$ and the exergy destruction in the NCZ, $Ex_{Q,destruction}$. Then, the equation of the exergy balance for the NCZ can be written as follows:

$$Ex_{out,NCZ} = \left[\begin{array}{c} Ex_{out,UCZ} + Ex_{Q,LCZ} \\ - (Ex_{Q,UCZ} + Ex_{Q,sidewalls}) \\ - Ex_{Q,destruction} \end{array} \right]_{NCZ} \quad (16)$$

The exergy efficiency of the NCZ is obtained by plugging the Eq. (16) in the Eq. (11):

$$\eta_{ex,NCZ} = \left(1 - \frac{Ex_{Q,UCZ} + Ex_{Q,sidewalls} + Ex_{Q,destruction}}{Ex_{out,UCZ} + Ex_{Q,LCZ}} \right)_{NCZ} \quad (17)$$

LCZ exergy efficiency. The desired exergy output from the LCZ - i.e the exergy accumulation in the LCZ $Ex_{Q,stored}$ - comes from the exergy transferred from the NCZ to the LCZ, $Ex_{out,NCZ}$; excluding the exergy loss from the LCZ to the NCZ, $Ex_{Q,NCZ}$, the exergy loss through the LCZ sidewalls, $Ex_{Q,sidewalls}$, the exergy loss through the LCZ bottom, $Ex_{Q,bottom}$ and the exergy destruction in the LCZ, $Ex_{Q,destruction}$. Then, the equation of the exergy balance for the NCZ can be written as follows:

$$\begin{aligned} Ex_{out,LCZ} &= (Ex_{Q,stored})_{LCZ} \\ &= \left[\begin{array}{c} Ex_{out,NCZ} \\ - (Ex_{Q,NCZ} + Ex_{Q,sidewalls} + Ex_{Q,bottom}) \\ - Ex_{Q,destruction} \end{array} \right]_{LCZ} \end{aligned} \quad (18)$$

The exergy efficiency of the NCZ is obtained by plugging the Eq. (18) in the Eq. (11):

$$\eta_{ex,LCZ} = \left(1 - \frac{Ex_{Q,NCZ} + Ex_{Q,sidewalls} + Ex_{Q,bottom} + Ex_{Q,destruction}}{Ex_{out,NCZ}} \right)_{NCZ} \quad (19)$$

A study carried out on a 4 m² SGSP showed – by measuring the temperatures every hour at different points in the pond, and at its bottom and on its insulated sidewalls – that the highest energy and exergy efficiencies were: 4.22% and 3.02% for the UCZ, 13.80% and 12.64% for the NCZ, and 28.11% and 27.45% for the LSZ, respectively in August under the climatic conditions of Adana, Turkey [66]. And it was found that exergy destruction and losses significantly affect pond performance and should be minimized to increase system efficiency.

7. RESULTS AND DISCUSSIONS

7.1 Constraints and economical savings

Given the low density of solar energy, very large collectors will be essential to collect significant quantities of energy. Thus, to replace a barrel of oil per day, an “ideal” collector must exceed a hundred square meters in surface! while taking into account the loss of energy on the way which will link the collector with the energy beneficiary. Therefore, under “realistic” conditions, this technique requires large investments including the construction, equipment, operation and of course the maintenance of such a large surface. [Thus, it became clear that very small ponds (less than 10,000 m²) are not so practical and economical (especially since pumps and instrumentation are less expensive for large installations). A 10,000 m² SGSP will therefore be effective for the production of heat, while that of the order of 100,000 m², for the production of electricity.

Almost half of the pond construction costs goes to lining cost. If salt can be provided for free (or at least cheaply) and the cost of land omitted, then we can spend capital more easily in the operation and maintenance process. Similarly, the larger the pond, the more these expenses will decrease. A solar pond that can be filled with seawater, residual brine after desalination and salt-work bittern will save resources and reduce investment costs, and also avoid possible pollution of coastal waters by brine and bittern [64]. However, seawater and bittern very easily become turbid during the SGSP operation, requiring more maintenance and turbidity control.

After carrying out the first stage of this the project, i.e. the stage of construction and installations, the cost of thermal energy will become directly related to the operating and maintenance expenses. This makes a solar pond with a surface area of more than 10,000 m², in a sunny zone (near the equator), a good competitor to oil. A modest-sized solar pond can provide process heat at medium temperatures (50-90 °C) at a unit cost cheaper than natural gas or coal. A design of a 23,240 m² SGSP, with a 1.8 m thick NCZ, for preheating water used in washing copper cathodes at a mining operation in Sierra Gorda, Chile, shows that reductions of 77% in diesel and 38% in the cost of energy could be anticipated [67].

The low power heat in the solar pond could also be applied to generate electricity using a heat pipe turbine or an Organic Rankine Cycle Engine (ORCE) (Figure 21). But here the economic results become less satisfactory. Heat engines operating at moderate temperatures have low thermodynamic efficiencies. Then organic operating fluids that have lower boiling points such as halocarbons (e.g. freon) or

hydrocarbons (e.g. propane) will be needed [19]. Maximum revenue can be achieved by maximizing engine hours or running at base load, given the relatively high cost of Organic Rankine Cycle generation equipment. But we must not forget that the economic results can be improved in sunny sites, and for large ponds of more than 100,000 m², if heat losses are well controlled and if the impact of the environmental costs of fossil fuels combustion is taken into account. The generating heat pipe turbines produced one hundred watts of electrical power from water at 54°C. The association of turbine with a solar pond leads to a competitive process heat and electricity supplier for the industry [68]. An experimental 5 kW heat pipe turbine for use with a solar pond has been developed and manufactured in Australia [69].

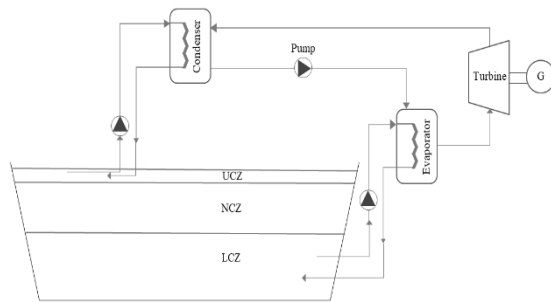


Figure 21. Schematic of a solar pond using an ORCE to generate power

7.2 Ecological savings

Solar ponds can reduce fuel consumption and greenhouse gas radiation in the rural industries demanding of process heating. They can be applied in commercial sector such as water supply for desalination, salt production, aquaculture, grain drying, fruit and vegetable drying and canning, dairy industry, etc. [68]. They ensure the option of an unchanged terrestrial heat balance, while avoiding any problem of excessive diffusion of CO₂ in the atmosphere, production of waste, or other environmental problems due to the combustion of fuel oil for example.

8. CONCLUSIONS

In this paper, we have proposed to design a salinity-gradient solar pond in Beirut, Lebanon, to alleviate the severity of the economic crisis and the difficulty of obtaining electricity for the different sectors of the country, including the industrial one. For this, a study was carried out on the different stages of the project, starting by presenting the geographical and meteorological characteristics of Beirut – which announced the possibility of establishing the project and its effectiveness – then, presenting similar designs that were previously established and proven effective. Next, we moved on to the engineering and construction phase, where we presented all the construction and instrumentation stages, and the methods of energy extraction, while continuing to benefit from the successful experiences mentioned previously. Later, we discussed the advanced stages of the project in terms of operation, maintenance and control, mentioning the theoretical and material resources required. We concluded the study with an overview of the economic aspect of the project and the difficulties it may face, which limit its competition with the available alternatives.

This project could be a preliminary test of solar pond technology in Lebanon, creating the small-scale pond detailed in the study in the suburbs of Beirut. If it succeeds, and it is undoubtedly thanks to the availability of the necessary geographical and meteorological factors, this technology will not only be able to support the Lebanese economy and partially save it from this crisis, but also to bring the agricultural sector out of its limits and neglect – especially, since the Bekaa Valley is good ground for this experience, and the coastal plains to the north and south as well. In addition, we do not neglect the possibility of benefiting from these ponds at the daily life level for individuals and groups in terms of heating, cooling and electricity production.

REFERENCES

- [1] Ranjan, K.R., Kaushik, S.C. (2014). Thermodynamic and economic feasibility of solar ponds for various thermal applications: A comprehensive review. *Renewable and Sustainable Energy*, 32: 123-139. <https://doi.org/10.1016/j.rser.2014.01.020>
- [2] Monjezi, A.A., Campbell, A.N. (2016). A comprehensive transient model for the prediction of the temperature distribution in a solar pond under mediterranean conditions. *Solar Energy*, 135: 297-307. <https://doi.org/10.1016/j.solener.2016.06.011>
- [3] Garg, H.P. (2012). *Advances in solar energy technology: Volume 3 Heating, agricultural and photovoltaic applications of solar energy*. Springer Science & Business Media. <https://doi.org/10.1007/978-94-017-0659-9>
- [4] Kurt, H., Halici, F., Binark, A.K. (2000). Solar pond conception—experimental and theoretical studies. *Energy Conversion and Management*, 41(9): 939-951. [https://doi.org/10.1016/S0196-8904\(99\)00147-8](https://doi.org/10.1016/S0196-8904(99)00147-8)
- [5] Kurt, H., Ozkaymak, M., Binark, A.K. (2006). Experimental and numerical analysis of sodium-carbonate salt gradient solar-pond performance under simulated solar-radiation. *Applied Energy*, 83(4): 324-342. <https://doi.org/10.1016/j.apenergy.2005.03.001>
- [6] Ganguly, S., Date, A., Akbarzadeh, A. (2019). On increasing the thermal mass of a salinity gradient solar pond with external heat addition: A transient study. *Energy*, 168: 43-56. <https://doi.org/10.1016/j.energy.2018.11.090>
- [7] Amigo, J., Meza, F., Suárez, F. (2017). A transient model for temperature prediction in a salt-gradient solar pond and the ground beneath it. *Energy*, 132: 257-268. <https://doi.org/10.1016/j.energy.2017.05.063>
- [8] Jayadev, T.S., Edesess, M. (1980). *Solar pond costs and performance, solar pond applications, solar ponds*. Solar Energy Research Institute, Golden, Colorado, 80401: 17-29.
- [9] Burston, I. (1996). *Application of salinity gradient solar ponds in salt affected areas of Victoria*. Masters by Research, RMIT University, Australia.
- [10] Saleh, A., Qudeiri, J.A., Al-Nimr, M.A. (2011). Performance investigation of a salt gradient solar pond coupled with desalination facility near the Dead Sea. *Energy*, 36(2): 922-931. <https://doi.org/10.1016/j.energy.2010.12.018>
- [11] Farrokhi, M., Jaefarzadeh, M.R., Bawahab, M., Faqeha, H., Akbarzadeh, A. (2022). Integration of a solar pond in

- a salt work in Sabzevar in Northeast Iran. *Solar Energy*, 244: 115-125. <https://doi.org/10.1016/j.solener.2022.08.032>
- [12] Caruso, G., Naviglio, A. (1999). A desalination plant using solar heat as a heat supply, not affecting the environment with chemicals. *Desalination*, 122(2-3): 225-234. [https://doi.org/10.1016/S0011-9164\(99\)00043-0](https://doi.org/10.1016/S0011-9164(99)00043-0)
- [13] Duffie, J.A., Beckman, W.A. (2013). *Solar Engineering of Thermal Processes*. John Wiley & Sons.
- [14] Kumar, A., Kishore, V.V.N. (1999). Construction and operational experience of a 6000 m² solar pond at Kutch, India. *Solar Energy*, 65(4): 237-249. [https://doi.org/10.1016/S0038-092X\(98\)00134-0](https://doi.org/10.1016/S0038-092X(98)00134-0)
- [15] Lu, H., Walton, J.C., Swift, A.H. (2001). Desalination coupled with salinity-gradient solar ponds. *Desalination*, 136(1-3): 13-23. [https://doi.org/10.1016/S0011-9164\(01\)00160-6](https://doi.org/10.1016/S0011-9164(01)00160-6)
- [16] Rabl, A., Nielsen, C.E. (1975). Solar ponds for space heating. *Solar Energy*, 17(1): 1-12. [https://doi.org/10.1016/0038-092X\(75\)90011-0](https://doi.org/10.1016/0038-092X(75)90011-0)
- [17] Ranjan, K.R., Kaushik, S.C. (2014). Thermodynamic and economic feasibility of solar ponds for various thermal applications: A comprehensive review. *Renewable and Sustainable Energy Reviews*, 32: 123-139. <https://doi.org/10.1016/j.rser.2014.01.020>
- [18] Akbarzadeh, A., Golding, P. (1992). The importance of wall angle for stability in solar ponds. *Solar Energy*, 49(2): 123-126. [https://doi.org/10.1016/0038-092X\(92\)90146-2](https://doi.org/10.1016/0038-092X(92)90146-2)
- [19] El-Sebaili, A.A., Ramadan, M.R.I., Aboul-Enein, S., Khallaf, A.M. (2011). History of the solar ponds: A review study. *Renewable and Sustainable Energy Reviews*, 15(6): 3319-3325. <https://doi.org/10.1016/j.rser.2011.04.008>
- [20] Lu, H., Swift, A.H., Hein, H.D., Walton, J.C. (2004). Advancements in salinity gradient solar pond technology based on sixteen years of operational experience. *Solar Energy Engineering*, 126: 759-767. <https://doi.org/10.1115/1.1667977>
- [21] Leblanc, J., Akbarzadeh, A.A. (2011). Heat extraction methods from salinity-gradient solar ponds and introduction of a novel system of heat extraction for improved efficiency. *Solar Energy*, 85: 3103-3142. <https://doi.org/10.1016/j.solener.2010.06.005>
- [22] Silva, G., Almanza, R. (2009). Use of clays as liners in solar ponds. *Solar Energy*, 83: 905-919. <https://doi.org/10.1016/j.solener.2008.12.008>
- [23] Robbins, M.C., Lu, H., Swift, A.H.P. (1995). Investigation of the suitability of a geosynthetic clay liner system for the EL paso solar pond. *Proceedings of the 1995 Annual Conference of American Solar Energy Society*, Campbell-Howe R., Wilkins Crowder B., eds. Minneapolis, MN, pp. 63-68.
- [24] Reid, R.L., Swift, A.H.P. (1989). Design, construction, and initial operation of a 3,355 m² solar pond in El paso. *Solar Energy Engineering*, 111: 330-337. <https://doi.org/10.1115/1.3268331>
- [25] Lichtwardt, M.A., Remmers, H. (1995). Advanced solar pond liner technologies, joint fall meeting of the texas sections of APS and AAPT, and SPS zone 13, Lubbock, Texas.
- [26] Lichtwardt, M.A., Comer, A.I. (1997). Geosynthetics in salinity-gradient solar ponds. *IFAI Geotechnical Fabrics Report*, 15(3): 24-28.
- [27] Andrew, J., Akbarzadeh, A.A. (2002). Solar pond project: Stage 1 - Solar pond for industrial process heating. End of Project Report for Project Funded Under Renewable Energy Commercialization Program Australia Greenhouse Office, RMIT University, Melbourne.
- [28] Lu, H. (1994). Monitoring and data analysis for solar pond operation. Master's Thesis, The University of Texas at El Paso, El Paso, TX.
- [29] Lu, H., Swift, A.H.P. (1996). Reconstruction and operation of the El paso solar pond with a geosynthetic clay liner system. In: Davidson J., Chavez J. (Eds.), *Solar Engineering – Proceedings of ASME International Solar Energy Conference*, San Antonio, TX.
- [30] Busquets, E., Kumar, V., Lu, H. (2012). Thermal analysis and measurement of a solar pond prototype to study the non-convective zone salt gradient stability. *Solar Energy*, 86: 1366-1377. <https://doi.org/10.1016/j.solener.2012.01.029>
- [31] Tundee, S., Singh, R., Akbarzadeh, A.A. (2010). Heat extraction from salinity-gradient solar ponds using heat pipe heat exchangers. *Solar Energy*, 84: 1706-1716. <https://doi.org/10.1016/j.solener.2010.04.010>
- [32] Akbarzadeh, A.A., MacDonald, R.W.G., Wang, Y.F. (1983). Reduction of surface mixing in solar ponds by floating rings. *Solar Energy*, 31: 377-380. [https://doi.org/10.1016/0038-092X\(83\)90136-6](https://doi.org/10.1016/0038-092X(83)90136-6)
- [33] Bezir, N.Ç., Dönmez, O., Kayali, R., Özek, N. (2008). Numerical and experimental analysis of a salt gradient solar pond performance with or without reflective covered surface. *Applied Energy*, 85: 1102-1112. <https://doi.org/10.1016/j.apenergy.2008.02.015>
- [34] Bozkurt, I., Karakilcik, I., Dincer, I. (2014). Energy efficiency assessment of integrated and nonintegrated solar ponds. *International Journal of Low-Carbon Technologies*, 9: 45-51. <https://doi.org/10.1093/ijlct/cts052>
- [35] Erden, M., Karakilcik, M., Dincer, I. (2017). Performance investigation of hydrogen production by the flat-plate collectors assisted by a solar pond. *International Journal of Hydrogen Energy*, 42: 2522-2529. <https://doi.org/10.1016/j.ijhydene.2016.04.116>
- [36] Alcaraz, A., Valderrama, C., Cortina, J.L., Akbarzadeh, A.A. (2018). Increasing the storage capacity of a solar pond by using solar thermal collectors: Heat extraction and heat supply processes using in-pond heat exchangers. *Solar Energy*, 171: 112-121. <https://doi.org/10.1016/j.solener.2018.06.061>
- [37] Atiz, A., Karakilcik, H., Erden, M., Karakilcik, M. (2019). Investigation energy, exergy and electricity production performance of an integrated system based on a low-temperature geothermal resource and solar energy. *Energy Conversion and Management*, 195: 798-809. <https://doi.org/10.1016/j.enconman.2019.05.056>
- [38] Ghaebi, H., Rostamzadeh, H. (2020). Performance comparison of two new cogeneration systems for freshwater and power production based on organic Rankine and Kalina cycles driven by salinity-gradient solar pond. *Renewable Energy*, 156: 748-767. <https://doi.org/10.1016/j.renene.2020.04.043>
- [39] Edesess, M., Benson, D., Henderson, J., Jayadev, T.S. (1979). Economic and performance comparisons of salty and saltless solar ponds (No. SERI/TP-35-213). National Renewable Energy Lab. (NREL), Golden, CO (United

- States).
- [40] Karim, C., Jomâa, S.F., Akbarzadeh, A.A. (2011). A laboratory experimental study of mixing the solar pond gradient zone. *Solar Energy*, 85: 404-417. <https://doi.org/10.1016/j.solener.2010.10.010>
- [41] Hull, J.R., Bushnell, D.L., Sempsrote, D.G., Pena, A. (1989). Ammonium sulfate solar pond: Observations from small-scale experiments. *Solar Energy*, 43: 57-64. [https://doi.org/10.1016/0038-092X\(89\)90100-X](https://doi.org/10.1016/0038-092X(89)90100-X)
- [42] Liao, Y., Swift, A.H.P., Reid, R.L. (1988). Determination of the critical froude number for gradient establishment in a solar pond. In: Murphy L.M., Mancini T.R. (Eds.), *Solar Engineering*. Denver, CO, pp. 101-105.
- [43] Zangrado, F., Johnstone, H.W. (1988). Effect of injection parameters on gradient formation. In: Murphy L.M., Mancini T.R., (Eds.), *Solar Engineering*, Denver, CO, pp. 95-99.
- [44] Valderrama, C., Akbarzadeh, A.A., Cortina, J.L. (2011). Solar energy storage by salinity gradient solar pond: pilot plant construction and gradient control. *Desalination*, 279: 445-450. <https://doi.org/10.1016/j.desal.2011.06.035>
- [45] Ding, L.C., Akbarzadeh, A.A., Date, A. (2016). Transient model to predict the performance of thermoelectric generators coupled with solar pond. *Energy*, 103: 271-289. <https://doi.org/10.1016/j.energy.2016.02.124>
- [46] Zangrado, F. (1991). On the hydrodynamics of salt-gradient solar ponds. *Solar Energy*, 46: 323-341. [https://doi.org/10.1016/0038-092X\(91\)90048-2](https://doi.org/10.1016/0038-092X(91)90048-2)
- [47] Xu, H., Golding, P., Swift, A.H.P. (1991). Method for monitoring stability within a solar pond gradient. Second ASME-JSES-JSME International Solar Energy Conference, Reno, NV, USA *Solar Engineering*, pp. 75-82.
- [48] Xu, H., Nielson, C.E., Golding, P. (1987). Prediction of internal stability within a salinity gradient solar pond. In: Huacuz V.J.M. et al. (Eds.), *Proceedings of International Conference on Progress in Solar Ponds*, Cuernavaca Morelos, Mexico, pp. 107-117.
- [49] Bryant, H.C., Colbeck, I. (1977). A solar pond for London? *Solar Energy*, 19: 321-322. [https://doi.org/10.1016/0038-092X\(77\)90079-2](https://doi.org/10.1016/0038-092X(77)90079-2)
- [50] Kooi, C.F. (1979). The steady state salt gradient solar pond. *Solar Energy*, 23: 37-45. [https://doi.org/10.1016/0038-092X\(79\)90041-0](https://doi.org/10.1016/0038-092X(79)90041-0)
- [51] Hawlader, M.N.A. (1980). The influence of the extinction coefficient on the effectiveness of solar ponds. *Solar Energy*, 25: 461-464. [https://doi.org/10.1016/0038-092X\(80\)90454-5](https://doi.org/10.1016/0038-092X(80)90454-5)
- [52] Hawlader, M.N.A. (1981). An analysis of the non-convecting solar pond. *Solar Energy*, 27: 195-204. [https://doi.org/10.1016/0038-092X\(81\)90121-3](https://doi.org/10.1016/0038-092X(81)90121-3)
- [53] Sodha, M.S., Kaushik, N.D., Rao, S.K. (1981). Thermal analysis of three zone solar pond. *Energy Research*, 5: 321-340. <https://doi.org/10.1002/er.4440050404>
- [54] Bansal, P.K., Kaushik, N.D. (1981). Salt gradient stabilized solar pond collector. *Energy Conversion and Management*, 21: 81-95. [https://doi.org/10.1016/0196-8904\(81\)90010-8](https://doi.org/10.1016/0196-8904(81)90010-8)
- [55] Brown, S.T., Cambel, A.B. (1982). Net energy analysis of residential solar ponds. *Energy*, 7: 457-463. [https://doi.org/10.1016/0360-5442\(82\)90055-X](https://doi.org/10.1016/0360-5442(82)90055-X)
- [56] Beniwal, R.S., Singh, R.V., Chaudhary, D.R. (1985). Heat losses from a salt-gradient solar pond. *Applied Energy*, 19: 273-285. [https://doi.org/10.1016/0306-2619\(85\)90002-9](https://doi.org/10.1016/0306-2619(85)90002-9)
- [57] Hassab, M.A., El-Masry, O.A. (1991). Effects of edges on solar-energy collection in small solar ponds. *Applied Energy*, 38: 81-94. [https://doi.org/10.1016/0306-2619\(91\)90067-8](https://doi.org/10.1016/0306-2619(91)90067-8)
- [58] Kayali, R., Bozdemir, S., Kiyamac, K. (1998). A rectangular solar pond model incorporating empirical functions for air and soil temperatures. *Solar Energy*, 63: 345-353. [https://doi.org/10.1016/S0038-092X\(98\)00104-2](https://doi.org/10.1016/S0038-092X(98)00104-2)
- [59] Jaefarzadeh, M.R. (2004). Thermal behavior of a small salinity-gradient solar pond with wall shading effect. *Solar Energy*, 77: 281-290. <https://doi.org/10.1016/j.solener.2004.05.013>
- [60] Karakilcik, M., Dincer, I., Rosen, M.A. (2006). Performance investigation of a solar pond. *Applied Thermal Engineering*, 26: 727-735. <https://doi.org/10.1016/j.applthermaleng.2005.09.003>
- [61] Karakilcik, M., Kıymaç, K., Dincer, I. (2006). Experimental and theoretical temperature distributions in a solar pond. *International Journal of Heat and Mass Transfer*, 49: 825-835. <https://doi.org/doi.org/10.1016/j.ijheatmasstransfer.2005.09.026>
- [62] Kaushik, S.C., Ranjan, K.R., Panwar, N.L. (2013). Optimum exergy efficiency of single-effect ideal passive solar stills. *Energy Efficiency*, 6: 595-606. <https://doi.org/10.1007/s12053-013-9194-x>
- [63] Karakilcik, M., Dincer, I., Bozkurt, I., Atiz, A. (2013). Performance assessment of a solar pond with and without shading effect. *Energy Conversion and Management*, 65: 98-107. <https://doi.org/10.1016/j.enconman.2012.07.001>
- [64] Li, N., Yin, F., Sun, W., Zhang, C., Shi, Y. (2010). Turbidity study of solar ponds utilizing seawater as salt source. *Solar Energy*, 84: 289-295. <https://doi.org/10.1016/j.solener.2009.11.010>
- [65] Andrews, J., Akbarzadeh, A. (2005). Enhancing the thermal efficiency of solar ponds by extracting heat from the gradient layer. *Solar Energy*, 78(6): 704-716. <https://doi.org/10.1016/j.solener.2004.09.012>
- [66] Karakilcik, M., Dincer, I. (2008). Exergetic performance analysis of a solar pond. *International Journal of Thermal Sciences*, 47: 93-102. <https://doi.org/10.1016/j.ijthermalsci.2007.01.012>
- [67] Garrido, F., Vergaraa, J. (2013). Design of solar pond for water preheating used in the copper cathodes washing at a mining operation at Sierra Gorda, Chile. *Renewable and Sustainable Energy*, 5(4): 043103. <https://doi.org/10.1063/1.4812652>
- [68] Chinn, A., Akbarzadeh, A.A., Andrews, J. (2001). Solar pond technology and its role in salinity mitigation. *ISES Solar World Congress*, pp. 839-844.
- [69] Johnson, P., Akbarzadeh, A.A., Theurer, F., Nguyen, T., Mochizuki, M. (1996). Heat pipe turbine becoming a reality, heat pipe technology. *Theory, Applications and Prospects*, Actes du 5e Symposium international, Melbourne, Australia, 17-20 November 1996, Pergame, Oxford (1997).

NOMENCLATURE

B	gap width of the diffuser, m
Ex	exergy, W
Fr	Froud number, dimensionless
g	acceleration due to gravite, m.s^{-2}
G_S	rate of incident solar radiation, W.m^{-2}
Q	heat transfer, W
S	salinity, %
T	temperature of the system or individual zone, K
T_0	environment reference temoerature, K
T_s	surface temperature of the sun, K
v	injection velocity at the diffuser outlet, m.s^{-1}

z height of the pond, m

Greek symbols

ρ	density of the surrounding saline fluid, kg.m^{-3}
$\Delta\rho$	density difference between the injected fluid and the surrounding fluid, kg.m^{-3}
η	efficiency

Subscripts

e	energy
ex	exergy